minerals

MDPI

Article

Combined Influence of Low-Grade Metakaolins and Natural Zeolite on Compressive Strength and Heavy Metal Adsorption of Geopolymers

Alcina Johnson Sudagar [1,2,*], Slávka Andrejkovičová [1], Fernando Rocha [1], Carla Patinha [1], Maria R. Soares [3], Ana Luísa Velosa [4] and Eduardo Ferreira da Silva [1]

1 Geosciences Department, Geobiotec Research Unit, Campus Universitário de Santiago, University of Aveiro, 3810-193 Aveiro, Portugal; slavka@ua.pt (S.A.); tavares.rocha@ua.pt (F.R.); cpatinha@ua.pt (C.P.); eafsilva@ua.pt (E.F.d.S.)
2 Institute of Physical Chemistry, Polish Academy of Sciences, 01-224 Warsaw, Poland
3 CICECO & LCA, Campus Universitário de Santiago, University of Aveiro, 3810-193 Aveiro, Portugal; rosarios@ua.pt
4 Civil Engineering Department, RISCO, Campus Universitário de Santiago, University of Aveiro, 3810-193 Aveiro, Portugal; avelosa@ua.pt
* Correspondence: asudagar@ichf.edu.pl or sudagaralcinajohnson@gmail.com

Abstract: Metakaolins (MKs) prepared from low-grade kaolins located in the Alvarães (A) and Barqueiros (B) regions of Portugal were used as the aluminosilicate source to compare their effect on the compressive strength and heavy metal adsorption of geopolymers. Natural zeolite, an inexpensive, efficient adsorbent, was used as an additive in formulations to enhance geopolymers' adsorption capacities and reduce MK utilization's environmental footprint. Geopolymers were synthesized with the replacement of MK by zeolite up to 75 wt.% (A25, B25—25% MK 75% zeolite; A50, B50—50% MK 50% zeolite; A75, B75—75% MK 25% zeolite; A100, B100—100% MK). The molar ratios of SiO_2/Al_2O_3 and Na_2O/Al_2O_3 were kept at 1 to reduce the sodium silicate and sodium hydroxide environmental impact. Geopolymers' crystallography was identified using X-ray diffraction analysis. The surface morphology was observed by scanning electron microscopy to understand the effect of zeolite incorporation. Chemical analysis using X-ray fluorescence spectroscopy and energy dispersive X-ray spectroscopy yielded information about the geopolymers' Si/Al ratio. Compressive strength values of geopolymers obtained after 1, 14, and 28 days of curing indicate high strengths of geopolymers with 100% MK (A100—15.4 MPa; B100—32.46 MPa). Therefore, zeolite did not aid in the improvement of the compressive strength of both MK-based geopolymers. The heavy metal (Cd^{2+}, Cr^{3+}, Cu^{2+}, Pb^{2+}, and Zn^{2+}) adsorption tests exhibit relatively higher adsorption capacities of Barqueiros MK-based geopolymers for all the heavy metals except Cd^{2+}. Moreover, zeolite positively influenced divalent cations' adsorption on the geopolymers produced from Barqueiros MK as B75 exhibits the highest adsorption capacities, but such an influence is not observed for Alvarães MK-based geopolymers. The general trend of adsorption of the heavy metals of both MK-based geopolymers is $Pb^{2+} > Cd^{2+} > Cu^{2+} > Zn^{2+} > Cr^{3+}$ when fitted by the Langmuir isotherm adsorption model. The MK and zeolite characteristics influence geopolymers' structure, strength, and adsorption capacities.

Keywords: geopolymer; metakaolin; zeolite; heavy metals; adsorption; compressive strength; low grade

check for updates

Citation: Sudagar, A.J.; Andrejkovičová, S.; Rocha, F.; Patinha, C.; Soares, M.R.; Velosa, A.L.; Silva, E.F.d. Combined Influence of Low-Grade Metakaolins and Natural Zeolite on Compressive Strength and Heavy Metal Adsorption of Geopolymers. *Minerals* **2021**, *11*, 486. https://doi.org/10.3390/min11050486

Academic Editor: Alexander Mikhailovich Kalinkin

Received: 9 April 2021
Accepted: 29 April 2021
Published: 1 May 2021

Publisher's Note: MDPI stays neutral with regard to jurisdictional claims in published maps and institutional affiliations.

Copyright: © 2021 by the authors. Licensee MDPI, Basel, Switzerland. This article is an open access article distributed under the terms and conditions of the Creative Commons Attribution (CC BY) license (https://creativecommons.org/licenses/by/4.0/).

1. Introduction

Since the discovery of geopolymers in 1972 by Davidovits, the aluminosilicate-based materials found application in a wide range of fields [1]. Geopolymers have exhibited remarkable potential as sustainable cement replacements [2,3], adsorbents [4,5], and membrane filters [6,7]. Metakaolin (MK), the calcined form of the kaolin clay, is one of the most commonly used aluminosilicate sources besides fly-ash and ground granulated blast

furnace slag [8]. One prospective candidate to be incorporated in the geopolymer structure is zeolite, an inexpensive and natural source known for its excellent adsorption capacities. Zeolites found application as adsorbents, catalysts, and ion-exchangers because they encapsulate/trap many small molecules in their microporous structures [5,9,10]. Besides, they also have heat-insulating characteristics as they release zeolitic water on heating [11]. Therefore, incorporating zeolite into the geopolymer matrix would enhance the geopolymers' adsorption capacities and benefit concrete mixtures.

High compressive strength is an important performance attribute for geopolymers to be used as a replacement for Portland cement. Geopolymer compressive strength has to match the requirements of cement binders for concrete in real-life applications. Concrete compressive strength requirements for general construction vary from 17 MPa for residential construction to 28 MPa and higher for commercial and industrial structures. Some applications also require compressive strength of up to 70 MPa [12]. The ordinary Portland cement (OPC) is known to be produced in various grades with compressive strengths from 17 MPa to 53 MPa after 28 days of curing, with the most common high-grade OPC being OPC—33 (33 MPa at 28 days), OPC—43 (43 MPa at 28 days), and OPC—53 (53 MPa at 28 days) [13,14]. The concrete grade used in concrete preparation affects the final compressive strengths of the concrete. Research has extensively focused on different formulations of geopolymers to satisfy this requirement. However, the compressive strength is affected significantly along with other geopolymer properties by the MK characteristics and fillers' nature, besides the chemical activator ratios.

Secondly, the heavy metals and toxic compounds found in the waste effluents released from industries, agricultural, and household activities accumulate in our water bodies giving rise to dangerous repercussions. The dire need to find a solution to the toxic waste effluents problem instigated extensive research on efficient adsorbents. Along these lines, geopolymers found their use in heavy metal immobilization [15,16], and in adsorption of the heavy metal wastes such as Cd, Cr, Cu, Pb, and Zn [17]; ammonium [18]; and dyes [19] that are hazardous to the environment. The heavy-metal adsorption occurs through ion exchange of the heavy metal ions with the several ions present in the geopolymer surface. They are also adsorbed in the pores present on geopolymers [17].

Several kaolinitic clay deposits in Portugal charted out by Lopes et al. (2018) are currently unexplored due to a lack of industrial demand [20]. The Alvarães and Barqueiros region deposits are in the northwest part of Portugal, particularly in the littoral region between the Douro and Minho rivers. The Alvarães sedimentary kaolin deposits are located in the tectono-sedimentary basin of the Alvarães, southwest of Viana do Castelo in the Central Iberian Zone of the Hesperian Massif. This deposit consists of two distinctive types of kaolin, sedimentary and residual kaolin. Barqueiros is a sedimentary deposit composed of kaoliniferous sand layers located in the municipality of Barcelos [21]. This kaolin is extremely fine-grained. These kaolins are usually characterized by disordered structures and yellowish color, characteristics that other industries do not accept. However, a growing scientific and economic interest in using MKs in geopolymers is inducing MK production. Therefore, it is of paramount interest to understand the influence of the different Portuguese MKs on the geopolymer properties and how they affect the filler's influence as a replacement in the structure. In our previous study, high geopolymer strength and adsorption capacities for heavy metals were obtained for commercially available high-grade MK-based geopolymers with natural zeolite as a filler [22]. Further enhancement in the adsorption capacities was observed with the addition of cork industry waste [23]. Therefore, in the current work, the aim was to study the effect of different low-grade Portuguese MKs on the geopolymer properties such as compressive strength and heavy metal adsorption. Subsequently, changes in the strength and the heavy metal adsorption capacities of these geopolymers by the addition of a natural zeolite were investigated.

2. Materials and Methods

2.1. Materials Used for Geopolymerization

Geopolymers were prepared using the calcined form of low-grade kaolins from the Alvarães and Barqueiros regions of Portugal. The physical properties of these low-grade kaolins are shown in Table 1. Zeolite ($(Ca, K_2, Na_2, Mg)4Al_8Si_{40}O_{96}{\cdot}24H_2O$) (ZeoBau micro 50, from Nižný Hrabovec, Zeocem, Slovakia, CEC = 83 meq/100 g, SSA = 1663 m^2/kg, particle size 0–0.05 mm, bulk density = 500–600 $g{\cdot}dm^{-3}$) was used as a filler, as it is known to have a high specific surface area and cation exchange capacity. Additional information regarding the zeolite can be found at http://www.iza-online.org/natural/, accessed on 1 May 2021. Hydrated sodium silicate (Merck, Germany Merck, Germany; 8.5 wt.% Na_2O, 28.5 wt.% SiO_2, 63 wt.% H_2O, extra pure) was the silicon source, and sodium hydroxide (ACS AR Analytical Reagent Grade Pellets, purity 99.61%) acted as an alkaline activator for dissolution of aluminosilicate. The reaction was performed in water.

Table 1. Characteristics of low-grade kaolins from Portugal.

Features/Properties	Values	
	Alvarães	**Barqueiros**
Whiteness	65–75	75–85
Density (g/mL)	2.4–2.7	2.4–2.7
Oil Absorption	31–45	31–45
pH	4–7	5–8
Residue at 53 μm (%)	<0.5	<0.3
Water absorption (%)	23 ± 3 (1180 °C)	24 ± 3 (1220 °C)

2.2. Fabrication of Geopolymers

Alvarães (A) and Barqueiros (B) low-grade kaolins were dried in an oven at 50 °C for 24 h, then ground and calcined for 4 h at 750 °C to form MKs. Geopolymers were prepared according to Andrejkovičová et al. (2016) [22]. Reference geopolymers were based on pure MK (A100, B100). Blended geopolymers were prepared by replacing MK with 25, 50, and 75 wt.% of zeolite (A75, B75; A50, B50; and A25, B25, respectively). The molar oxide ratios kept to minimize the amount of chemicals in the geopolymerization process were as follows: $SiO_2/Al_2O_3 = 1$, $Na_2O/Al_2O_3 = 1$, $H_2O/Na_2O = 17$.

The following steps were involved in the preparation of geopolymers. Alkaline activators NaOH and hydrated sodium silicate were mixed in a water medium under stirring and then added to the MK and zeolite to dissolve them. The Heidolph ST-1 laboratory stirrer was used to mix aluminosilicates and alkali solutions at two different speeds, 100 rpm for 2 min and 200 rpm for 4 min, to homogenize the paste to avoid bubble formation. The stirred slurries were poured into 20 mm × 20 mm × 20 mm cubic molds, vibrated for 5 min to release the bubbles, and placed in the oven at 50 °C for 24 h. After this, the specimens were removed and left to cool at room temperature. The cubic geopolymer specimens were then immersed in plastic containers filled with tap water at room temperature and analyzed after 1 day, 14 days, and 28 days of curing. The specimens from each type of geopolymer were prepared in triplicates.

2.3. Methods

The methods used are in accordance with Andrejkovičová et al. (2016) [22]. The component materials of geopolymers, i.e., kaolinites and their corresponding MKs and zeolite, were analyzed using a PANalytical Axios X-ray fluorescence (XRF) spectrometer to understand their chemical composition. Mineralogical composition using X-ray diffraction (XRD) analysis for all base components and geopolymers was performed by the X'Pert-Pro M.P.D. Philips/ PANalytical model. The operating conditions were 30 mA and 50 kV. The scan was performed between 4° and 65° 2θ by using the Cu Kα radiation (λ = 1.5405 Å) at a speed of 0.02 °/s. The XRD phase detection was performed using the X'Pert HighScore

(PW3209) program.The morphological analysis of the base components was performed using the FEI Nova NanoSEM 450 scanning electron microscope in the range of 3–30 kV. The salient morphological features of geopolymers and their elemental composition were observed using the scanning electron microscope (SEM—Hitachi, SU 70) and energy dispersive X-ray spectrometer (EDS—EDAX with detector Bruker AXS, software: Quantax) operated at 3–30 kV.

The compressive strengths of the three cubic specimens (20 mm × 20 mm × 20 mm) from each geopolymeric formulation were tested using the (SHIMADZU: AG-IC 100 kN) universal testing machine after 1 day, 14 days, and 28 days of curing. The procedure was carried out with a maximum force of 5 kN at the speed of 50 N/s, as per the standard EN 1015-11 [24].

The adsorption of five heavy metal cations, Pb^{2+}, Zn^{2+}, Cu^{2+}, Cd^{2+}, and Cr^{3+}, on geopolymers was studied using the atomic absorption spectrometer (GBC Avanta). Batch adsorption experiments using nitrate solutions were performed in accordance with Andrejkovičová et al. (2016) [22]. In short, 20 mL of heavy metal solution was contacted with 200 mg of pretreated geopolymer for 7 hours. Then, the solution was centrifuged at 3500 rpm for 10 minutes, acidified, and analyzed.

3. Results and Discussion

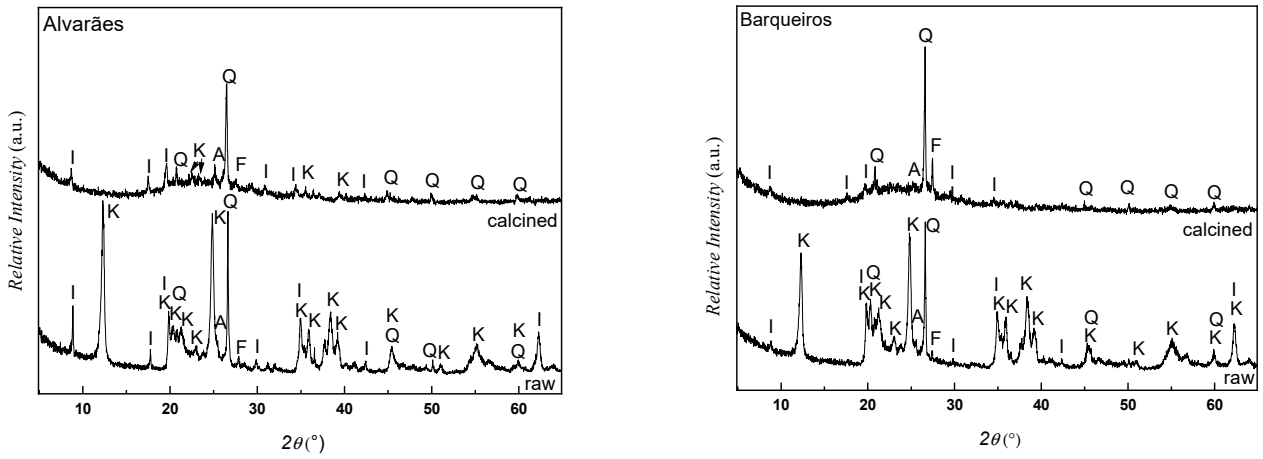
3.1. Characterization of Base Materials

3.1.1. X-Ray Diffraction (XRD) Analysis

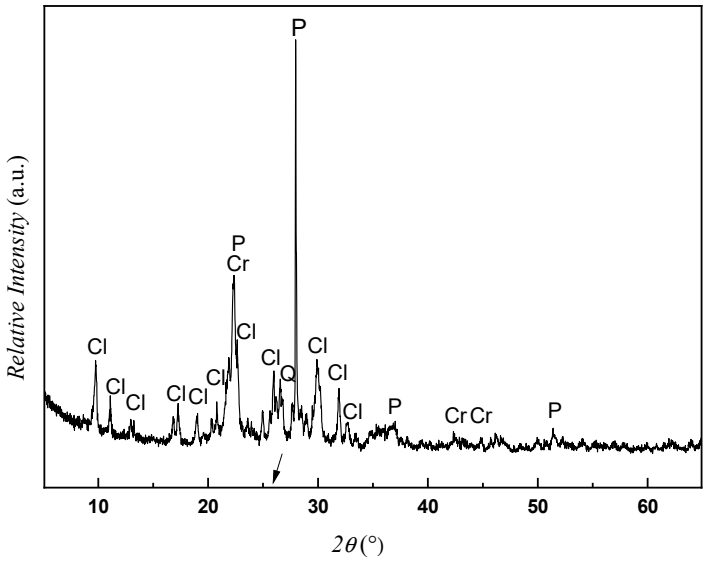
The mineralogical composition of low-grade kaolins, calcined kaolins, and zeolite is shown in Figure 1a,b. Both Alvarães and Barqueiros kaolins contain kaolinite ($Al_2Si_2O_5(OH)_4$) as the primary component along with small quantities of illite ((K, H_3O)(Al, Mg, Fe)$_2$(Si, Al)$_4O_{10}$[$(OH)_2$,(H_2O)]) a), quartz (SiO_2), anatase (TiO_2), and K-feldspar ($KAlSi_3O_8$) (Figure 1a).

XRD patterns of both calcined kaolins are very similar, consisting of a broad reflection centered at ~24° 2θ, representing the high amorphous contents obtained by transforming kaolinite into MK. Thermal treatment of kaolins caused kaolinite transformation into MK as most of the kaolinite reflections are not observed in calcined samples, unlike peaks of illite, quartz, anatase, and K-feldspar. (Figure 1a). Small kaolinite peaks are still visible for Alvarães kaolin after calcination, indicating incomplete transformation.

The significant component in the zeolite sample (Figure 1b) is clinoptilolite ((Na, K, Ca)$_{2\text{-}3}Al_3$(Al, Si)$_2Si_{13}O_{36}\cdot 12H_2O$). Admixtures include cristobalite (SiO_2), plagioclase ((Na, Ca)(Si, Al)$4O_8$), and quartz (SiO_2).



(**a**)



(**b**)

Figure 1. (**a**) XRD patterns of Alvarães and Barqueiros samples before (raw) and after calcination (calcined) (A—anatase, F—feldspar, I—illite, K—kaolinite, Q—quartz), (**b**) XRD patterns of zeolite (Cl—clinoptilolite, Cr—cristobalite, P—plagioclase, Q—quartz).

3.1.2. Chemical Analysis by X-ray Fluorescence (XRF)

The chemical analysis of the base materials helped determine the Si/Al ratio and, consequently, the amount of water required to prepare geopolymers (Table 2). High amounts of silicon and aluminum are observed in the kaolin samples. The SiO_2/Al_2O_3 ratio is higher than the standard value of 1.15 for both kaolins (1.16 and 1.27 for Alvarães and Barqueiros, respectively). This higher ratio is due to quartz, illite, and feldspar observed in the XRD diffractograms of the kaolins (Figure 1a). The Barqueiros kaolin contains higher impurities as compared to the Alvarães kaolin. Raw Alvarães and Barqueiros kaolins and zeolite have a higher loss on ignition (L.O.I.) due to the removal of surface-bound and structural water molecules. Increased Ti and K values are related to anatase and illite admixtures, respectively (Table 2, Figure 1a).

Table 2. The chemical analysis of geopolymer components.

Sample		Composition, wt. (%)									
		Na_2O	MgO	Al_2O_3	SiO_2	P_2O_5	K_2O	CaO	TiO_2	Fe_2O_3	L.O.I.
Alvarães	Kaolin	0.048	0.22	38.86	45.06	0.09	1.19	0.01	0.52	1.14	12.63
	MK	0.079	0.24	44.13	51.20	0.10	1.36	0.01	0.61	1.34	0.66
Barqueiros	Kaolin	0.057	0.25	36.92	46.92	0.10	1.16	0.05	0.37	1.17	12.83
	MK	0.092	0.30	41.97	53.39	0.12	1.38	0.06	0.42	1.32	0.79
Zeolite		0.314	0.85	12.07	70.61	0.04	3.66	3.39	0.20	1.78	6.89

Zeolite contains Al and Si primarily as expected; however, the SiO_2/Al_2O_3 ratio is quite different from kaolins. The zeolite's SiO_2/Al_2O_3 (5.85) ratio falls in the category of medium silica zeolites, which have a SiO_2/Al_2O_3 mass ratio in the range of 3.53–11.76, typical of clinoptilolite enriched with calcium. It was reported that the higher the SiO_2/Al_2O_3 mass ratio, the more hydrophobic the zeolite, and thus it will interact less with polar solvents such as water [25]. Elevated values of other elements, K and Ca, are associated with clinoptilolite. The Ca can also be related to anorthite ($CaAl_2Si_2O_8$) from the plagioclase feldspar series due to relatively lower quantities of Na (Table 2).

3.1.3. Morphology Characterization Using Scanning Electron Microscopy/Energy-Dispersive X-ray Spectroscopy (SEM/EDS)

The overall view of Alvarães kaolin exhibits flakes of kaolinite that are highly aggregated (Figure 2). The Barqueiros kaolin, differently, exhibits smaller aggregates and less aggregated fine flakes (Figure 3). This morphological difference could play a significant role in their reaction mechanism to form geopolymers. The impurities present in these kaolins could not be detected in SEM. The zeolite exhibits the needle-shaped aggregated structure (Figure 4). The thickness of these needles is a few tens of nanometers (Figure 4b).

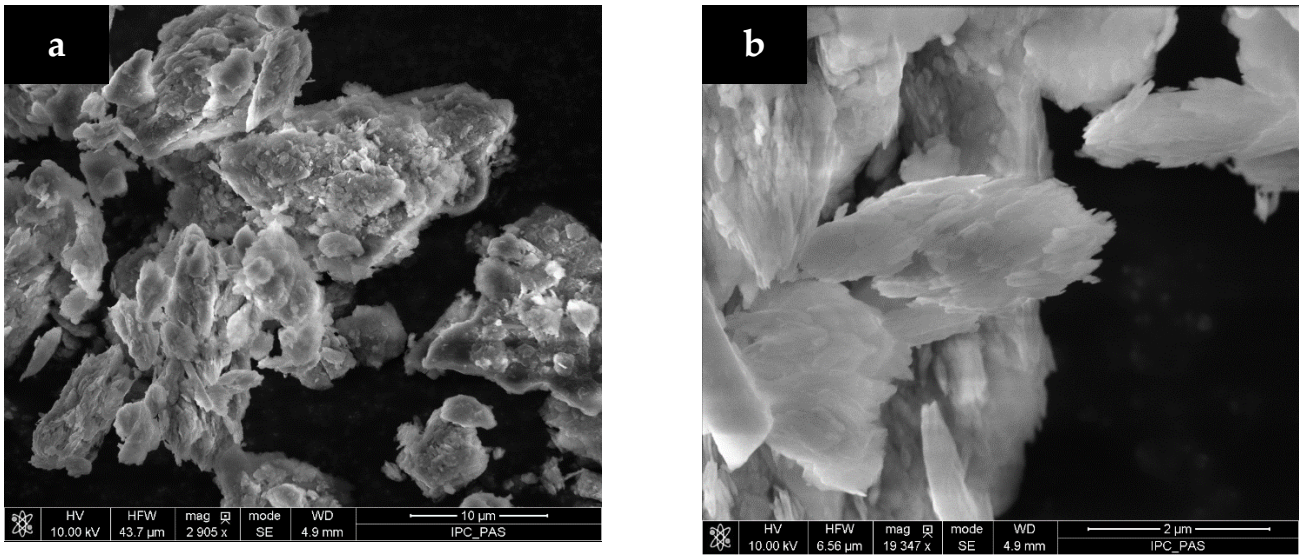


Figure 2. Morphological analysis of Alvarães kaolin.

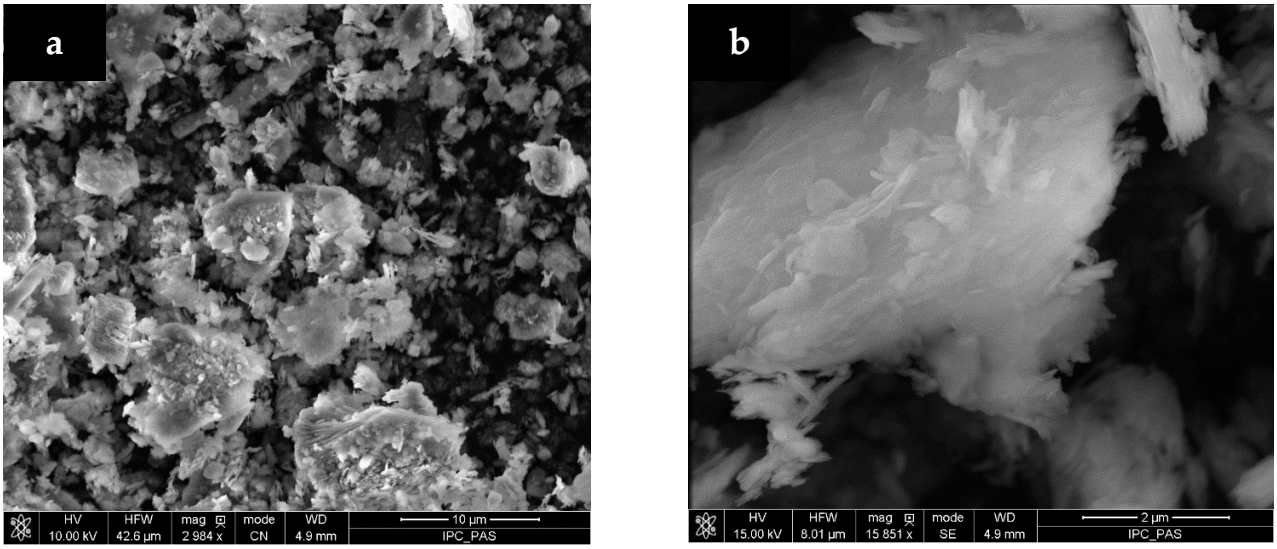


Figure 3. Morphological analysis of Barqueiros kaolin.

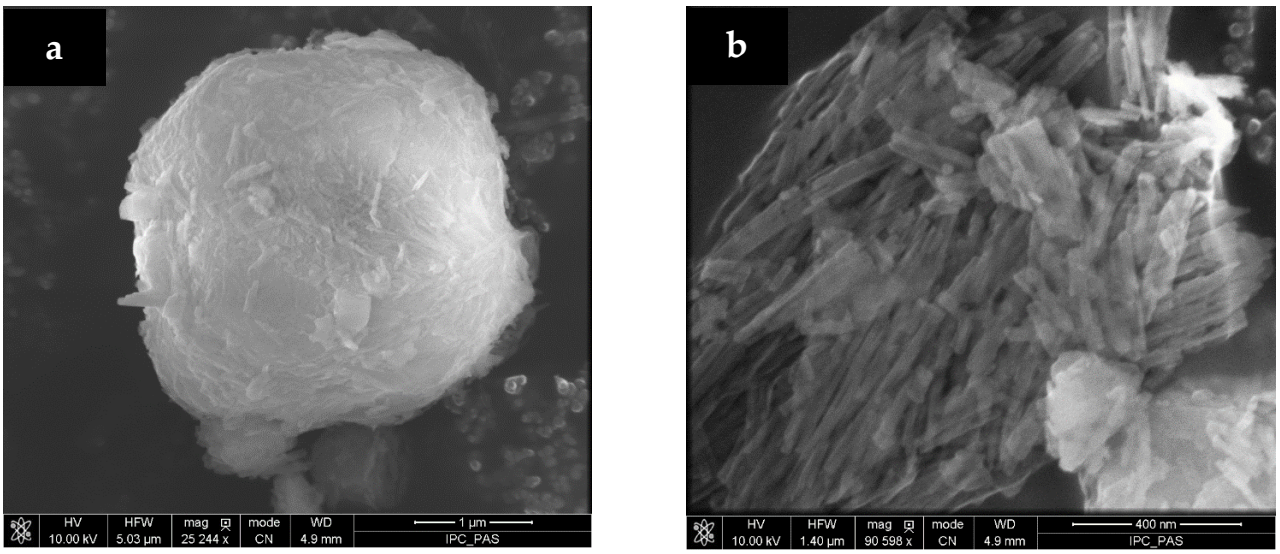


Figure 4. Morphological analysis of zeolite.

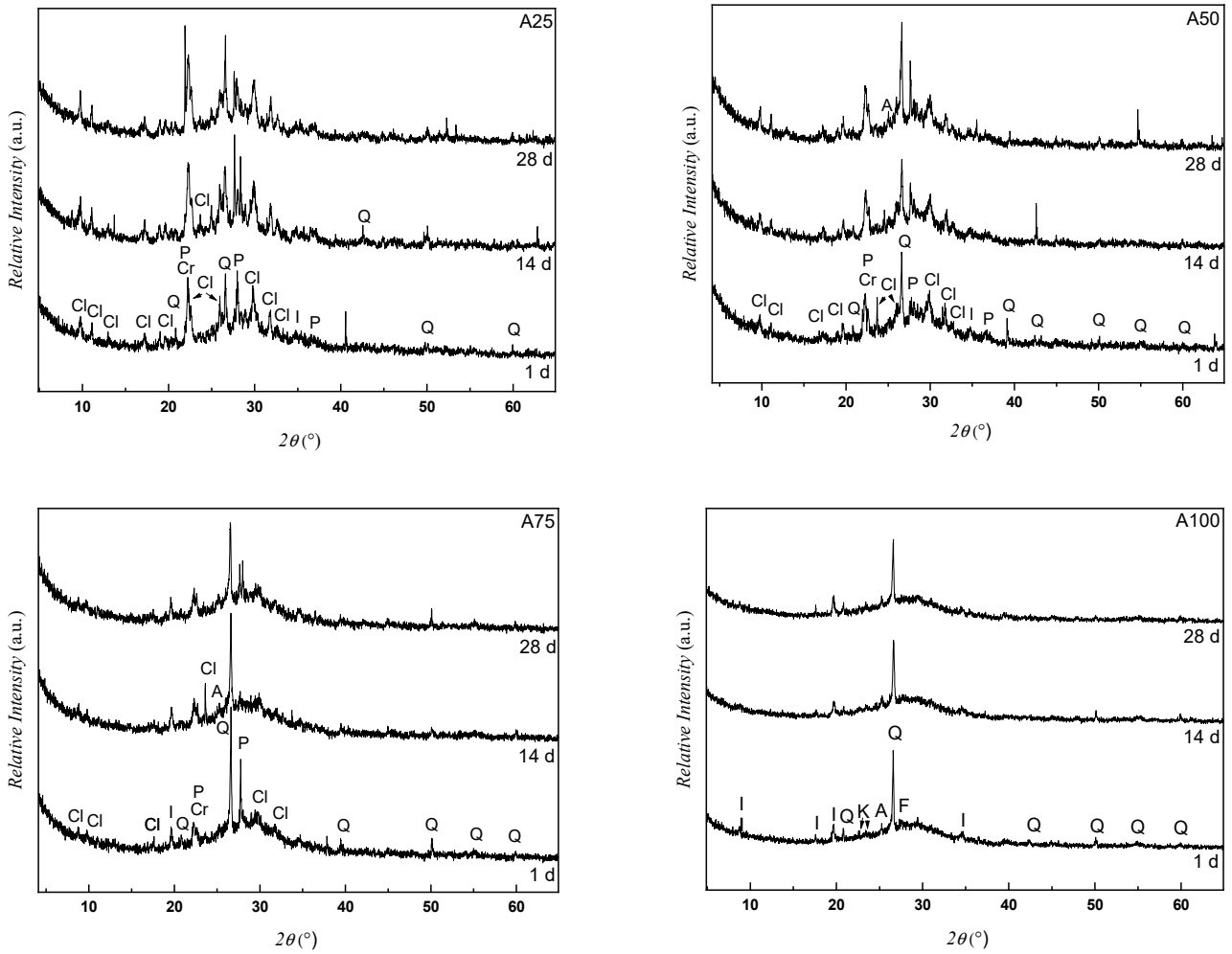
3.2. Characterization of Geopolymers

3.2.1. XRD Analysis

XRD analysis of geopolymers (Figure 5) was performed after 1 day, 14 days, and 28 days of curing to observe changes in their mineralogical composition. XRD patterns of geopolymers exhibit a characteristic broad band corresponding to the amorphous silicoaluminate framework obtained by activating MK by sodium hydroxide and sodium silicate. In both geopolymers, a higher amorphous nature is observed with increasing MK content from 25% to 100% in the structure evidenced by the growth in the broad band centering at ~28° 2θ. The broad band is the dominant characteristic of amorphous alkaline aluminosilicate, which decreases significantly with zeolite, indicating changes in the formed products' nature. Fewer kaolinitic peaks are observed in Alvarães MK-based geopolymer A100 than observed in the calcined kaolin component in Figure 1a. This disappearance indicates the dissolution of kaolinite during geopolymerization.

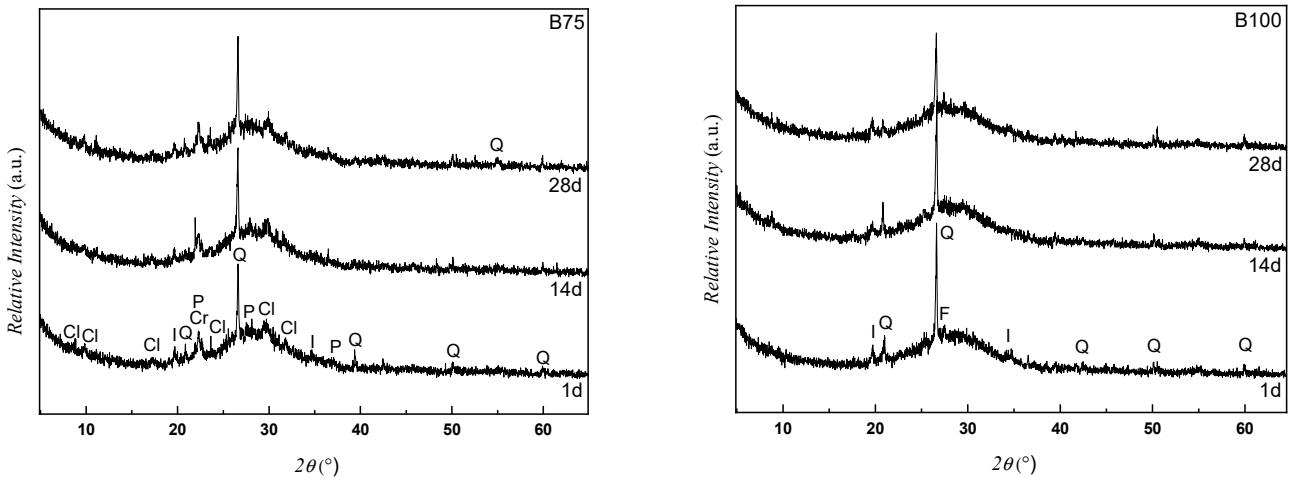
With increasing zeolite content in geopolymer formulation, more crystalline phases arise in their XRD patterns associated with clinoptilolite, plagioclase, and quartz. Anatase, feldspar, and quartz from the MK base materials are still clearly present in A100 and B100

geopolymers. Illite reflections are more noticeable in A100; however, the illite d_{001} peak at 8.8° 2θ disappears after one day of curing, indicating the structural decomposition of illite with curing time. Moreover, the formation of new minerals within all curing periods is not observed in the XRD diffractograms.



(**a**)

Figure 5. *Cont.*



(**b**)

Figure 5. XRD analysis of geopolymers from (**a**) Alvarães (A) and (**b**) Barqueiros (B) MKs after 1 day, 14 days, and 28 days of curing (A25, B25—25% MK 75% zeolite; A50, B50—50% MK 50% zeolite; A75, B75—75% MK 25% zeolite; A100, B100—100% MK).

3.2.2. SEM/EDS Analysis

SEM images of representative geopolymers A100, A50, B100, and B50 after 28 days of curing are referenced in Figures 6–9. Different formations can be identified in the case of geopolymers from Alvarães MK. Figure 6a through d shows the distinct morphology found in A100 geopolymer with 100% MK in the structure. This geopolymer consists of thin layered structures that are highly compacted. All the formations shown have a similar Si/Al ratio except for the particle x in Figure 6b, which has a higher amount of aluminum than silicon (Supplementary Materials, Figure S1). Figure 6b also exhibits a unique sheet type particle y, which has a high amount of potassium (Figure S2), thus indicating microcline, a potassium-rich alkali feldspar detected in XRD analysis (Figure 5). Spherical micropores can be observed on the surface, as in Figure 6a. Thin layers stacked together are also visible in Figure 6c with an Si/Al ratio similar to the bulk material (Figure S3).

The A50 geopolymer's morphology with 50% Alvarães MK—50% zeolite is shown in Figure 7a–d. The A50 geopolymer structure is more disordered as compared to the A100 geopolymer. It also exhibits spherical pores similar to those observed on the A100 geopolymer surface. Unique structures with different Si/Al ratios indicate different components like illite, quartz, and zeolite in the structure, besides the MK. Other elements present in the composition are Ca, K, Na, and Fe, which differ depending on the surface's components (Figures S4–S7). The thin layer sheet structure (Figure 7b), which has a high amount of K in its composition (Figure S4) compared to the surrounding environment, might be a feldspar. There are stacked layers rich in K and Na embedded between the geopolymer amorphous phase (Figure 7c,d, Figures S6 and S7), similar to that observed for A100 geopolymers (Figure 6). In Figure 7d, the layers also contain Mg and Fe, suggesting that these could be illite, whereas, in Figure 7c, the layers' chemical analysis by EDS suggests they are likely feldspar.

Figure 8a–c shows the distinctive features of the morphology of the Barqueiros MK-based geopolymer B100. The overall view in Figure 8a,b exhibits a compact surface with clusters of particles and large spherical micropores. The clusters appear to be aggregated particles of different sizes (Figure 8c and Figure S8). Unreacted thin layered structures or flakes are not observed in the B100 geopolymer, which could indicate a greater extent of geopolymerization, resulting in the least amount of unreacted phase. This effect could be due to the extremely fine nature of the Barqueiros kaolin (Figure 3) and higher amorphization observed in XRD (Figure 1a).

The B50 geopolymer with 50% MK and 50% zeolite, differently, exhibits a variety of morphological features, including pores, cleavages, thin layer sheets, and ball-like structures embedded in the geopolymer (Figure 9a–d). Thin layer sheets rich in K are representative of feldspar (Figure 9c and Figure S9). The ball-like embedded structure (Figure 9d and Figure S10) has very low Al relative to Si and significant amounts of Ca, K, and Fe, indicating that it could be an unreacted zeolite particle.

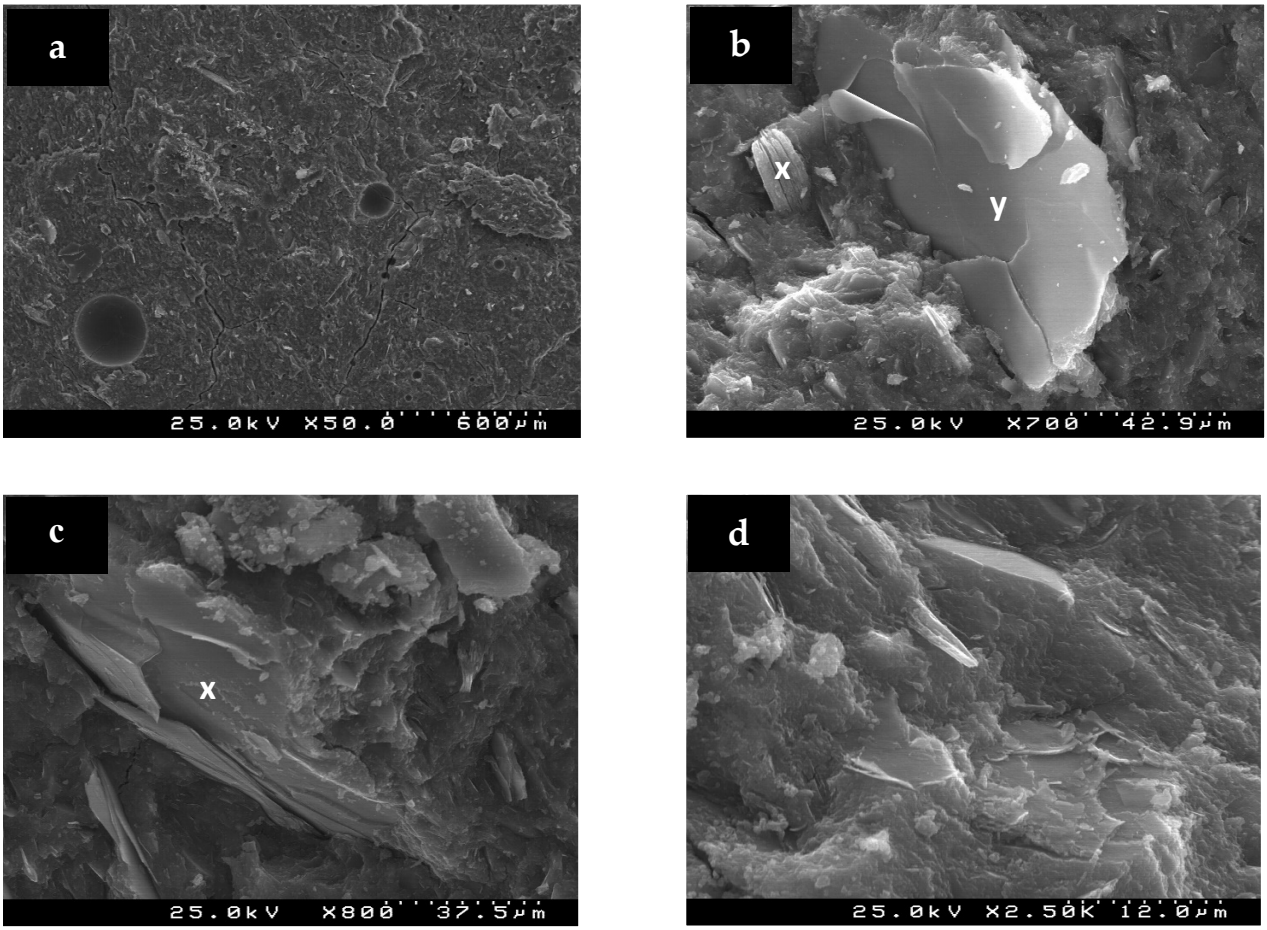


Figure 6. Morphological analysis of A100 (100% MK) Alvarães geopolymer.

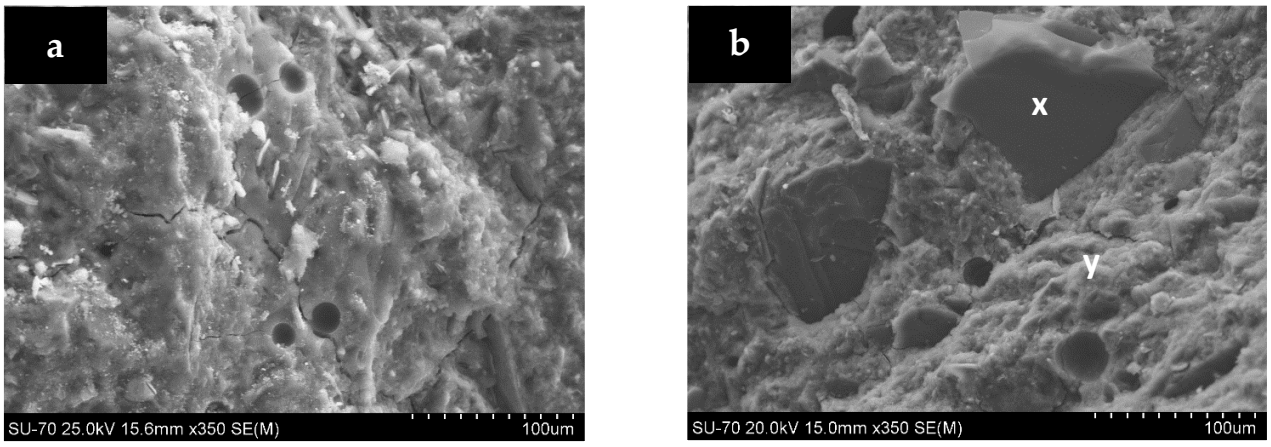


Figure 7. *Cont*.

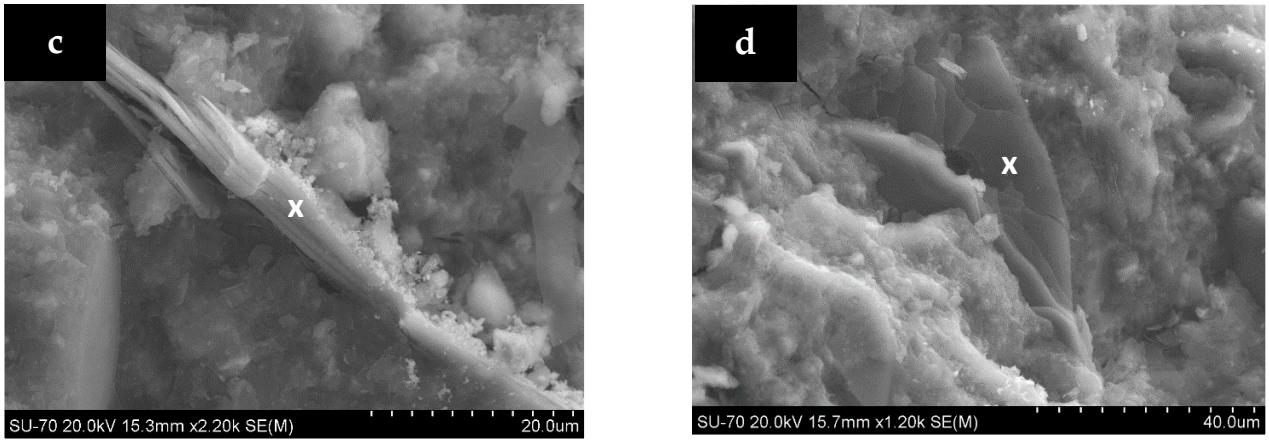


Figure 7. Morphological analysis of A50 (50% MK 50% zeolite) Alvarães geopolymer.

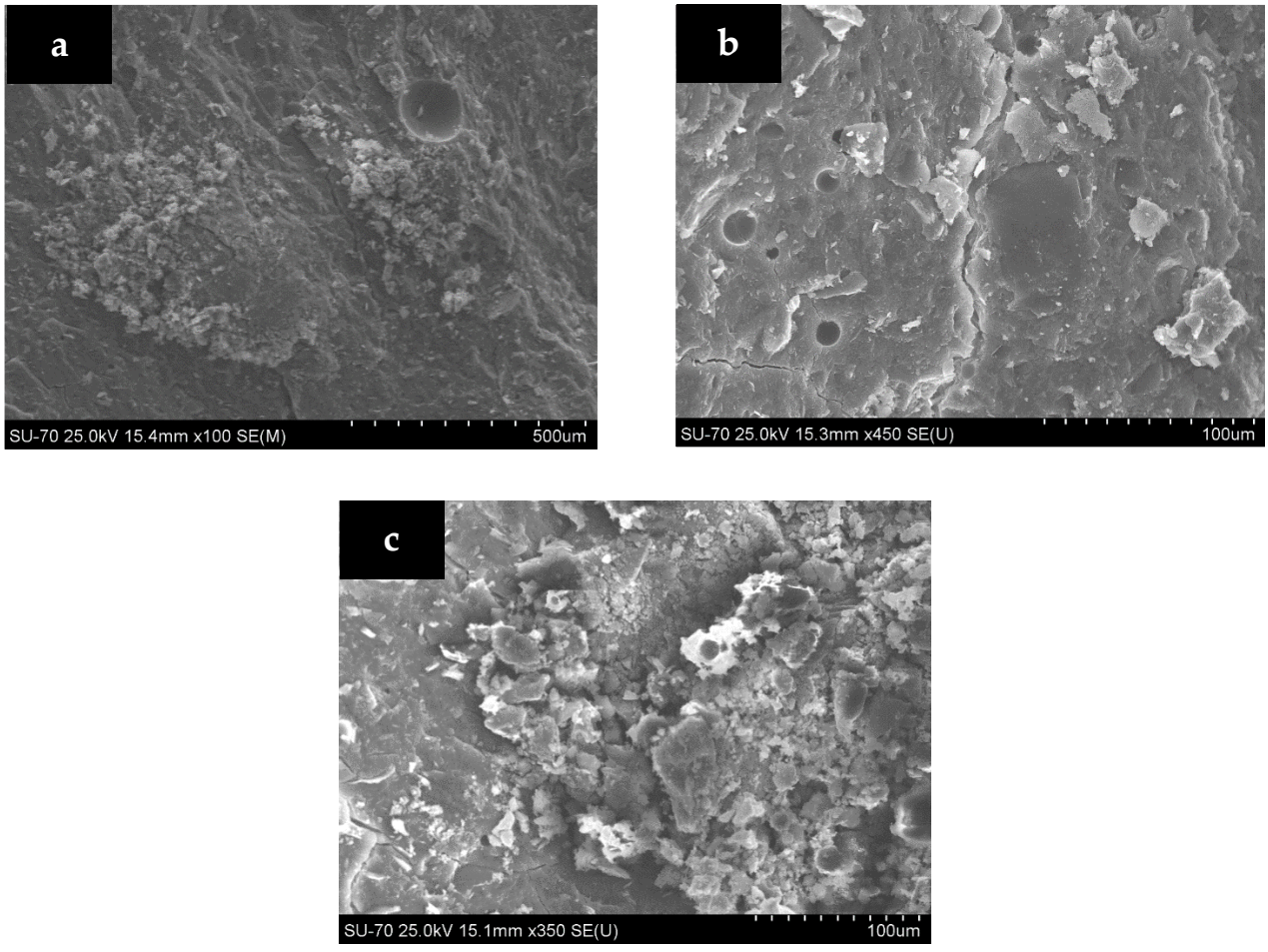


Figure 8. Morphological analysis of B100 (100% MK) Barqueiros geopolymer.

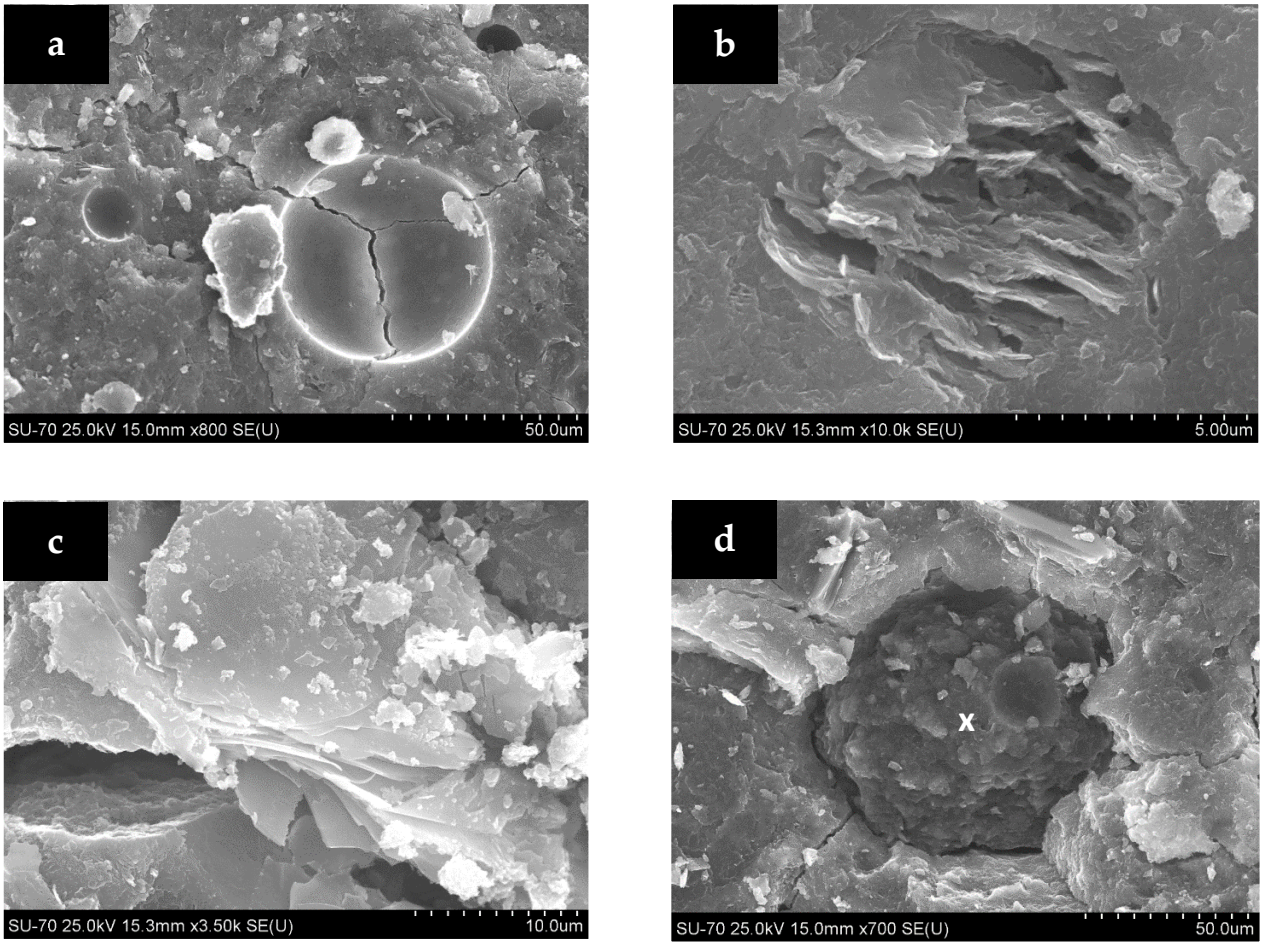


Figure 9. Morphological analysis of B50 (50% MK 50% zeolite) Barqueiros geopolymer.

3.2.3. Compressive Strength Rc

After curing for 1 day, 14 days, and 28 days, the compressive strength of geopolymers has given a wide range of values for the two different Portuguese MKs (Figure 10). Alvarães MK geopolymers exhibit increased strength from 1 to 28 days of curing time (Figure 10a). A100 exhibits the highest compressive strength value (15.4 MPa) after 28 days of curing due to the highest MK phase content, resulting in a greater extent of geopolymerization. The trend of increasing strength Rc of these Alvarães MK geopolymers is A25 < A75 $\leq$ A50 < A100. A50 and A75 reach after 28 days of curing very similar compressive strength values, 11.35 and 11.15 MPa, respectively. This indicates that the ratios of precursors, 50% MK/50% zeolite and 75% MK/25% zeolite, still provide a resistant geopolymer structure. The A25 geopolymer, differently, could not undergo an effective geopolymerization, as the MK content is too low, thereby providing poor strength (5.45 MPa at 28 days) of the structure.

The geopolymers from Barqueiros MK show higher Rc values than Alvarães MK geopolymers except for B25 (Figure 10). This superior strength is due to an improved geopolymerization state resulting from the higher extent of amorphization observed in XRD after calcining the kaolin (Figure 1a) and the extremely fine nature of the kaolin, which is less aggregated as observed in SEM (Figure 3). The maximum compressive strength is obtained for B100 geopolymer after 14 days (32.46 MPa) with a slight decrease (30.14 MPa) after 28 days. It is interesting to note that the Barqueiros MKs have higher strength even though the impurity content is higher, as seen in XRF (Table 2). The compressive strength of Barqueiros MK geopolymers increases with increasing MK in the structure (B25 < B50 < B75 < B100). The low MK content in the B25 geopolymer also significantly affected its

compressive strength, similar to the A25 geopolymer. The compressive strength of the Barqueiros MK geopolymer B100 is comparable to that of OPC—33, commonly used for residential constructions.

The Alvarães MK-based geopolymers exhibit lower compressive strengths than Barqueiros MK geopolymers, possibly due to the incomplete amorphization of the kaolinite (Figure 1a). Consequently, the MK available for geopolymerization is lower, leading to a less compact structure containing unreacted particles like stacked layers observed in SEM (Figures 6 and 7). The absence of such layers in Barqueiros MK geopolymer B100 (Figure 8) and a higher degree of amorphization of kaolinite (Figure 1a) lead to compact structures with greater strength. The addition of zeolite in the structure is effective for commercial MK-based geopolymers [22] but not very useful for the Portuguese MK-based geopolymers. However, it can still be concluded that the Portuguese MK-based geopolymers have improved compressive strength than commercial MK-based geopolymers reported by Andrejkovičová et al. (2016). The commercial MK geopolymer with 50% MK—50% zeolite (MK50) showed the highest compressive strength of 8.8 MPa after 28 days of curing [22]. The Portuguese MK geopolymers exhibit almost 2–4 times enhanced compressive strength. Therefore, the reactions occurring inside the geopolymers are dependent mainly on the MK used. Overall, Portuguese low-grade kaolins can be an excellent source of MK for geopolymers used as a replacement for cement.

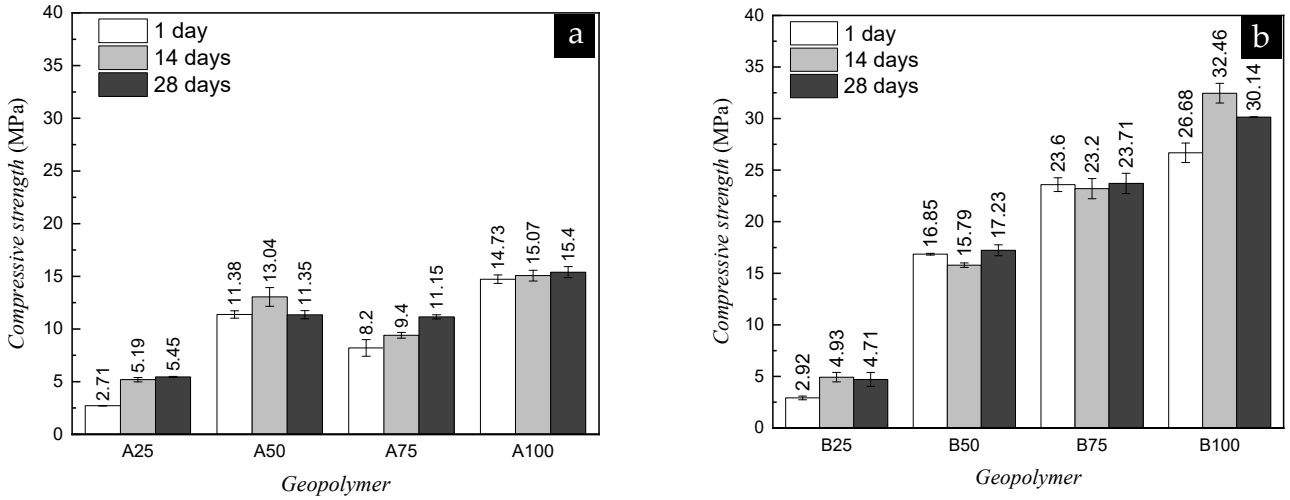


Figure 10. Compressive strength after 1 day, 14 days, and 28 days for geopolymers prepared from (**a**) Alvarães MK and (**b**) Barqueiros MK (A25, B25—25% MK 75% zeolite; A50, B50—50% MK 50% zeolite; A75, B75—75% MK 25% zeolite; A100, B100—100% MK).

3.2.4. Heavy Metal Adsorption

Adsorption of four divalent metal ions, lead, zinc, copper, and cadmium, and one trivalent metal ion, chromium, was tested on 28-day-cured Alvarães and Barqueiros MK-based geopolymers. The maximum adsorption capacity (Q) of geopolymers for each heavy metal is determined by the Langmuir isotherm model using the correlation between the quantity of heavy metal adsorbed (q) and the equilibrium concentration of the solution (C). The adsorption of Pb^{2+}, Cd^{2+}, Cu^{2+}, Zn^{2+}, and Cr^{3+} onto the Alvarães and Barqueiros MK geopolymers is shown in Figure 11. The fitting of the data is performed using the linear form of Langmuir isotherm with a high correlation factor R^2, indicating that the adsorption of heavy metal cations on geopolymer surface sites can be modeled using the monolayer adsorption model. The Langmuir constant (b) and maximum sorption capacity (Q) of geopolymers for heavy metals are represented in Table S1. Both Portuguese MK-based geopolymers have quite similar divalent cations' adsorption capacities; however, Barqueiros MK geopolymers are slightly superior except for Cd^{2+} (Figure 11).

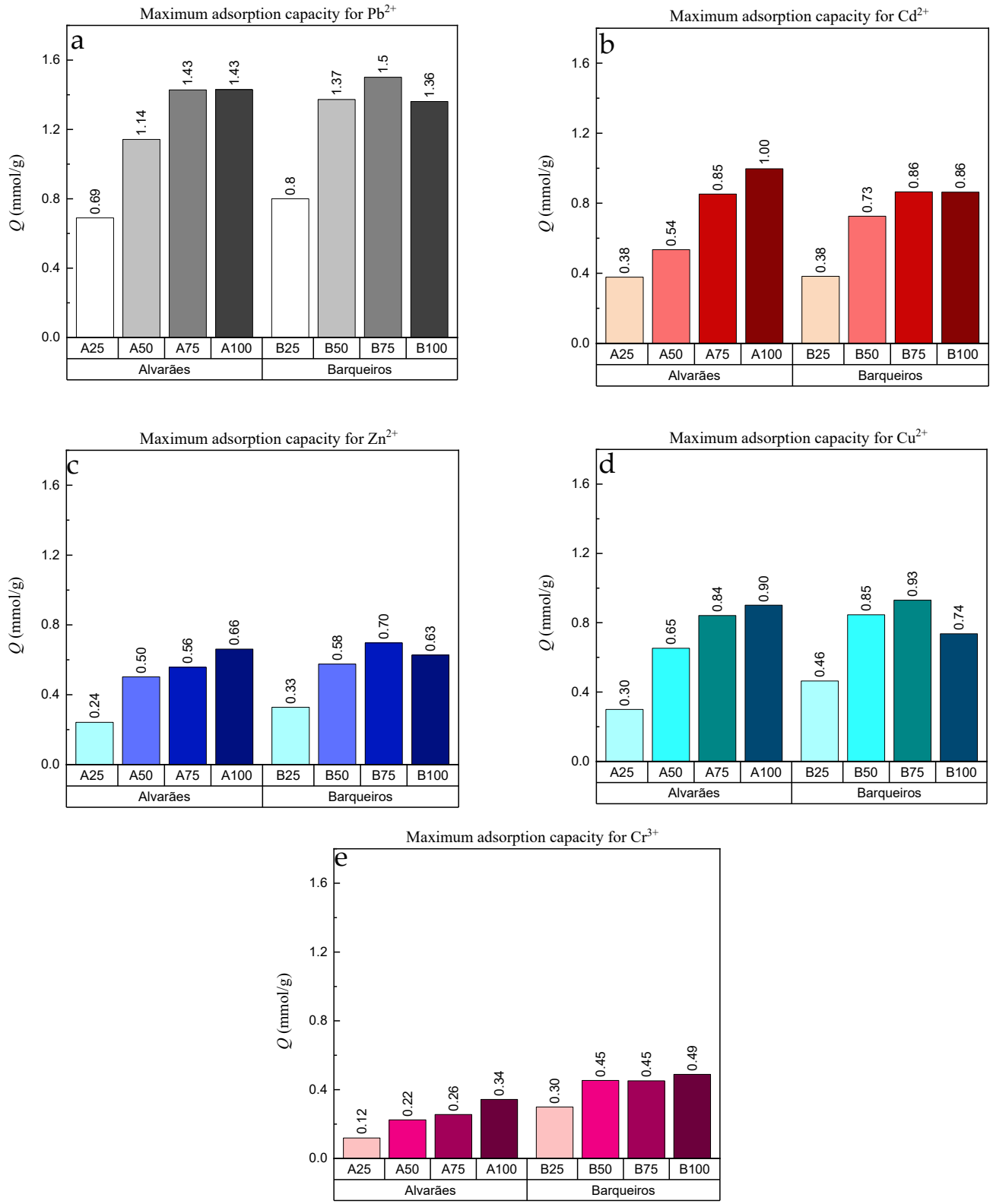


Figure 11. Maximum adsorption capacity of Alvarães and Barqueiros MK geopolymers for metal ions (**a**) Pb^{2+}, (**b**) Cd^{2+}, (**c**) Zn^{2+}, (**d**) Cu^{2+} and (**e**) Cr^{3+}. (A25, B25—25% MK 75% zeolite; A50, B50—50% MK 50% zeolite; A75, B75—75% MK 25% zeolite; A100, B100—100% MK).

(a) Adsorption of Pb^{2+}

The maximum adsorption capacity (Q) of Pb^{2+} is the highest for both the Portuguese MK-based geopolymers compared to other cations (Figure 11a). The Alvarães MK geopolymer exhibits higher Q with increasing MK in the structure from A25 (25% MK) to A75 (75% MK), and ultimately A75 (75% MK) and A100 (100% MK) geopolymers show almost similar adsorption capacity of 1.43 mmol/g. Contrastingly, the Barqueiros MK-based geopolymers exhibit increasing Q with increasing MK in the structure from B25 (25% MK) to B75 (75% MK), but B100 (100% MK) shows a relatively lower Q of 1.36 mmol/g as compared to B75, which has the highest Q of 1.5 mmol/g in the series. Zeolite's effect on Pb(II) adsorption is evident only for Barqueiros MK-based geopolymers. Although Pb(II) is adsorbed in relatively higher amounts than other heavy metals, the significantly lower values of Langmuir parameter 'b' (Table S1) indicated that this metal ion does not have a high affinity towards the geopolymers. Therefore, it is not as closely bound to the geopolymers as the other heavy metals.

(b) Adsorption of Cd^{2+}

The geopolymers exhibit the second-highest Q for Cd^{2+} cation. For this metal cation, the Alvarães MK geopolymers have relatively higher adsorption capacities (Figure 11b). The Q value for Alvarães MK geopolymers increases proportionally with the structure's MK ratio, as A100 (100% MK) showed the highest Q of 1.0 mmol/g. Barqueiros MK geopolymers also show an increase in the Q from B25 to B75. However, there is no further increase, and B75 and B100 have the same adsorption capacity of 0.86 mmol/g. For Cd^{2+} cation, the effect of zeolite in the structure is visibly not very prominent.

(c) Adsorption of Zn^{2+} and Cu^{2+}

For two metal cations, Zn^{2+} and Cu^{2+}, Alvarães MK geopolymers show an increasing trend of Q with increasing MK in the structure (A25 < A50 < A75 < A100), whereas the Barqueiros MK geopolymers exhibit the highest sorption Q for B75 with Q of 0.7 mmol/g for Zn^{2+} and 0.93 mmol/g for Cu^{2+} (Figure 11). The maximum adsorption obtained for Zn^{2+} and Cu^{2+} on A100 are 0.66 and 0.90 mmol/g, respectively. The zeolite affected Zn^{2+} and Cu^{2+} adsorption on Barqueiros MK geopolymers. This effect is similar to that observed for Pb^{2+} cation adsorption. The adsorption capacity trend of Barqueiros MK geopolymers for Zn(II) is B25 < B50 < B100 < B75 and for Cu(II) is B25 < B100 < B50 < B75.

The highly compact structure without any unreacted particles of B100 geopolymers could be an important reason for such low adsorption of divalent metal cations. The compact structure might be preventing access to exchange sites and also surface available for adsorption. The unreacted particles and pores could provide a greater surface area and better access to ion-exchange sites in the other geopolymers resulting in enhanced adsorption of heavy metal cations.

(d) Adsorption of Cr^{3+}

For the trivalent cation Cr^{3+}, the trend is similar for both the Portuguese MK-based geopolymers with increasing Q as MK increased in the geopolymer structure (Figure 11e). The Barqueiros MK geopolymer manifests higher Q (0.49 mmol/g for B100) than the Alvarães MK geopolymer (0.34 mmol/g for A100). However, the affinity of Cr(III) towards Alvarães MK geopolymers is significantly higher than Barqueiros MK geopolymers, apparent from the Langmuir parameter 'b' values. The trivalent heavy metal ion of Cr (III) is known to exist in complex ionic forms through complexation in water, and its state is susceptible to the pH of the system [26,27]. Therefore, it becomes challenging to adsorb this cation through the ion-exchange mechanism predominant for divalent metal cation adsorption onto the geopolymer surface.

The adsorption capacities of the heavy metal cations are in the order $Pb^{2+} > Cd^{2+} > Cu^{2+} > Zn^{2+} > Cr^{3+}$ which is quite similar to that for commercial MK-based geopolymers reported by Andrejkovičová et al. (2016) and Sudagar et al. (2018) [22,23]. This order is in reverse of the ionic potential of the metal cations.

3.2.5. Effect of Geopolymer Components on Heavy Metal Adsorption

Kaolinite has a low cation exchange capacity and small specific surface area; therefore, it shows low heavy metal adsorption capacities (Table 3). However, the calcination of this aluminosilicate source leads to a higher surface availability for adsorption. Simultaneously, the natural zeolite filler is known for its high surface area and ion exchange capacity. When geopolymerization gives rise to an amorphous matrix consisting of efficient adsorbents, the formation of new exchange sites in addition to the pre-existing ones results in significantly enhanced adsorption capacities of geopolymers. Therefore, geopolymers have better heavy metal adsorption capacities than the base components, kaolinite and zeolite (Table 3).

Low-grade MK-based geopolymers reported in this study exhibit higher adsorption capacities for all heavy metals under study except Zn (II) compared to zeolite and MK geopolymers reported in the literature (Table 3). The adsorption capacity of MK-based geopolymers reported by Kara et al. (2017) for Zn (II) is higher (1.14 mmol/g) than the adsorption capacities of Alvarães (0.66 mmol/g) and Barqueiros (0.70 mmol/g) MK geopolymers [28].

Barqueiros MK geopolymers exhibit the highest adsorption capacity for the ratio with 75% MK and 25% zeolite (B75), whereas Alvarães MK geopolymers show the highest *Q* for 100% MK geopolymer (A100). In the previous study on commercial MK geopolymers, the 75% MK and 25% zeolite ratio (MK75) geopolymer, and 100% MK (MK100) geopolymer, exhibited similar and the highest adsorption capacities [22]. Therefore, conclusively, the effect of zeolite in the structure is dependent on the MK used, based on this current study of the adsorption capacities of Portuguese MK geopolymers and a previous study on commercial MK-based geopolymers.

The overall view shows that the Portuguese MK geopolymers are effective adsorbents for heavy metal adsorption and perform better as compared to commercial MK-based geopolymers reported by Andrejkovičová et al. (2016) [22].

Table 3. Comparison of heavy metal adsorption capacities of geopolymers and the base components.

Heavy Metal	Adsorbent	Treatment	Source	Temperature (°C)	Time (h)	*Q* (mmol/g)	Reference
Pb(II)	Natural zeolite	Raw	-	-	3	0.30	[29]
		NaOH treated	-	-	3	0.48	
		Raw	Croatia	20	24	0.38	[30]
		NaCl treated	Croatia	20	24	0.44	
		NaCl treated	Croatia	70	24	0.58	
		Raw	-	RT	24	0.03	[31]
		Mg-Zeolite	-	23	-	0.28	[32]
	Natural kaolinite	Raw	-	22	4	0.39	[33]
		NaCl treated	-	22	4	0.59	
		H_2O_2 treated	USA	30	48	0.03	[34]
		Heat-treated	China	30	1	0.01	[35]
		Raw	Jordan	22	24	0.06	[36]
		Acid treated	Jordan	22	24	0.25	
		Surface modified	Jordan	22	24	0.26	
	Geopolymer	Raw	USA	30	3	0.05	[37]
		H_2SO_4 treated	USA	30	3	0.06	
		MK	-	25	24	0.71	[26]
		Commercial MK-zeolite	-	RT	7	1.26	[22]
		Alvarães MK-zeolite	-	RT	7	1.43	This study
		Barqueiros MK-zeolite	-	RT	7	1.50	
Cu(II)	Natural zeolite	Raw	Anatolia	25	5.5	0.14	[38]
		Raw	Bulgaria	constant	4	0.11	[39]
		Raw	Greece	22	6	0.09	[40]
		Raw	-	RT	24	0.06	[31]
		Raw	Serbia	20	24	0.13	[41]
		Mg modified zeolite	-	23	-	0.24	[32]
	Natural kaolinite	Raw	Turkey	25	2	0.17	[42]
		Heat-treated	China	30	1	0.02	[35]
		Raw	USA	30	6	0.14	[37]
		H_2SO_4 treated	USA	30	6	0.16	
	Geopolymer	MK	-	25	24	0.77	[26]
		Zeolite tuff	-	25	24	0.52	[43]
		Commercial MK-zeolite	-	RT	7	0.70	[22]
		Alvarães MK-zeolite	-	RT	7	0.90	This study
		Barqueiros MK-zeolite	-	RT	7	0.93	

Table 3. *Cont.*

Heavy Metal	Adsorbent	Treatment	Source	Temperature (°C)	Time (h)	Q (mmol/g)	Reference
Zn(II)	Natural zeolite	Raw	Anatolia	25	5.5	0.13	[38]
		Raw	Greece	22	6	0.05	[40]
		Raw	Turkey	25	5.5	0.34	[10]
	Natural kaolinite	Raw	-	RT	24	0.04	[31]
		Heat-treated	China	25	1	0.097	[44]
		MK	-	25	24	1.14	[28]
	Geopolymer	Zeolite tuff	-	25	24	0.41	[43]
		Commercial MK-zeolite	-	RT	7	0.55	[22]
		Alvarães MK-zeolite	-	RT	7	0.66	This study
		Barqueiros MK-zeolite	-	RT	7	0.70	
Cd(II)	Natural zeolite	Raw	-	-	3	0.53	[29]
		NaOH treated	-	-	3	0.62	
		Raw	Croatia	20	24	0.12	[30]
		NaCl treated	Croatia	20	24	0.21	
		Raw	-	RT	24	0.03	[31]
		Mg modified zeolite	-	23	-	0.33	[32]
		Raw	Greece	22	6	0.04	[40]
	Natural kaolinite	Raw	USA	30	4	0.09	[37]
		H_2SO_4 treated	USA	30	4	0.10	
		Raw	USA	30	4	0.06	[45]
		Poly(hydroxo zirconium) modified	USA	30	4	0.05	
		Tetrabutylammonium modified	USA	30	4	0.06	
		H_2O_2 treated	USA	30	48	0.08	[34]
		Heat-treated	China	30	1	0.008	[35]
	Geopolymer	MK	-	25	24	0.60	[26]
		Zeolite tuff	-	25	24	0.39	[43]
		Commercial MK-zeolite	-	RT	7	0.87	[22]
		Alvarães MK-zeolite	-	RT	7	1.00	This study
		Barqueiros MK-zeolite	-	RT	7	0.86	

4. Conclusions

1. The highest compressive strength is obtained for 100% MK geopolymers (A100—15.4 MPa; B100—32.46 MPa after 28 and 14 days of curing, respectively). The Barqueiros MK imparts higher compressive strength to the geopolymer structure than Alvarães MK because of Barqueiros kaolin's greater calcination extent. Natural zeolite lowers the compressive strength probably because of unreacted crystalline phases introduced in the geopolymer matrix.
2. The B100 geopolymer surface appears compact and without unreacted thin-layered structure particles, validating the higher degree of geopolymerization in MK geopolymers due to the extremely fine nature and effective calcination of Barqueiros kaolin.
3. Portuguese MK-based geopolymers show the highest adsorption capacity for Pb(II) and the adsorption trend is $Pb^{2+} > Cd^{2+} > Cu^{2+} > Zn^{2+} > Cr^{3+}$. Barqueiros MK geopolymers' adsorption capacity is higher than that of Alvarães MK geopolymers for all cations except Cd(II).
4. The optimal composition for Barqueiros MK geopolymers is 25% zeolite—75% MK (B75), and for Alvarães MK geopolymer is 100% MK (A100) for the highest adsorption capacity of heavy metals.
5. The effect of zeolite addition on the geopolymer strength and adsorption capacities depends on the type of MK used. Nonetheless, Portuguese MK-based geopolymers have higher compressive strengths and adsorption capacities as compared to commercial MK-based geopolymers. Therefore, low-grade kaolins can be attractive alternatives to high-grade commercial kaolins as construction materials and adsorbents.

Supplementary Materials: The following are available online at https://www.mdpi.com/article/10.3390/min11050486/s1, Figure S1. EDS analysis of particle x in Figure 6b, Figure S2. EDS analysis of particle y in Figure 6b, Figure S3. EDS analysis of particle x in Figure 6c, Figure S4. EDS analysis of particle x in Figure 7b, Figure S5. EDS analysis of particle y in Figure 7b, Figure S6. EDS analysis of particle x in Figure 7c, Figure S7. EDS analysis of particle x in Figure 7d, Figure S8. EDS analysis of particles in Figure 8c, Figure S9. EDS analysis of particles in Figure 9c, Figure S10. EDS analysis of particle x in Figure 9d. Table S1: Langmuir coefficients for the adsorption of cations onto Alvarães

and Barqueiros MK based geopolymers (A25, B25—25% MK 75% zeolite; A50, B50—50% MK 50% zeolite; A75, B75—75% MK 25% zeolite; A100, B100—100% MK).

Author Contributions: Conceptualization, A.J.S. and S.A.; formal analysis, A.J.S. and S.A.; funding acquisition; F.R.; methodology, A.J.S. and S.A.; writing—original draft preparation, A.J.S.; writing—review and editing, A.J.S. and S.A.; experiments and analysis, A.J.S., C.P., M.R.S., A.L.V., and E.F.d.S.; supervision, S.A. and F.R. All authors have read and agreed to the published version of the manuscript.

Funding: This research was supported by UIDB/4035/2020.

Acknowledgments: The authors are grateful to Zeocem a.s, Bystré, Slovakia, for providing zeolite used in this study. The author affiliated with the Polish institute would like to acknowledge the European Union's Horizon 2020 research and innovation programme under the Marie Skłodowska-Curie grant agreement No. 711859 and the financial resources for science in the years 2017–2022 awarded by the Polish Ministry of Science and Higher Education for the implementation of an international co-financed project.

Conflicts of Interest: There is no conflict of interest to declare.

References

1. Davidovits, J. *Geopolymer Chemistry and Applications*, 5th ed.; Davidovits, J., Ed.; Institut Géopolymère: Saint-Quentin, France, 2020.
2. Assi, L.N.; Carter, K.; Deaver, E.; Ziehl, P. Review of availability of source materials for geopolymer/sustainable concrete. *J. Clean. Prod.* **2020**, *263*, 121477. [CrossRef]
3. Ma, C.-K.; Awang, A.Z.; Omar, W. Structural and material performance of geopolymer concrete: A review. *Constr. Build. Mater.* **2018**, *186*, 90–102. [CrossRef]
4. Han, L.; Wang, J.; Liu, Z.; Zhang, Y.; Jin, Y.; Li, J.; Wang, D. Synthesis of fly ash-based self-supported zeolites foam geopolymer via saturated steam treatment. *J. Hazard. Mater.* **2020**, *393*, 122468. [CrossRef] [PubMed]
5. Minelli, M.; Papa, E.; Medri, V.; Miccio, F.; Benito, P.; Doghieri, F.; Landi, E. Characterization of novel geopolymer—Zeolite composites as solid adsorbents for CO_2 capture. *Chem. Eng. J.* **2018**, *341*, 505–515. [CrossRef]
6. Chen, H.; Zhang, Y.J.; He, P.Y.; Li, C.J.; Li, H. Coupling of self-supporting geopolymer membrane with intercepted Cr(III) for dye wastewater treatment by hybrid photocatalysis and membrane separation. *Appl. Surf. Sci.* **2020**, *515*, 146024. [CrossRef]
7. He, P.Y.; Zhang, Y.J.; Chen, H.; Han, Z.C.; Liu, L.C. Low-cost and facile synthesis of geopolymer-zeolite composite membrane for chromium(VI) separation from aqueous solution. *J. Hazard. Mater.* **2020**, *392*, 122359. [CrossRef] [PubMed]
8. Zhang, P.; Zheng, Y.; Wang, K.; Zhang, J. A review on properties of fresh and hardened geopolymer mortar. *Compos. Part B Eng.* **2018**, *152*, 79–95. [CrossRef]
9. Li, Y.; Li, L.; Yu, J. Applications of Zeolites in Sustainable Chemistry. *Chem* **2017**, *3*, 928–949. [CrossRef]
10. Yuna, Z. Review of the Natural, Modified, and Synthetic Zeolites for Heavy Metals Removal from Wastewater. *Environ. Eng. Sci.* **2016**, *33*, 443–454. [CrossRef]
11. Rożek, P.; Król, M.; Mozgawa, W. Geopolymer-zeolite composites: A review. *J. Clean. Prod.* **2019**, *230*, 557–579. [CrossRef]
12. National Ready Mixed Concrete Association. *Concrete in practice, in CIP 35-Testing Compressive Strength of Concrete*; National Ready Mixed Concrete Association: Silver Sring, MD, USA, 2003.
13. Strength of Cement. Concrete Technology 2020. Available online: https://buildingresearch.com.np/services/ct/ct2.php#:~{}:text=Grades%20mentioned%20in%20the%20cement,will%20be%20of%2053%20MPa (accessed on 9 June 2020).
14. Mathur, R.; Misra, A.K.; Goel, P. *Strength of Concrete vs. Grades of Cement*; NBM Media Pvt. Ltd.: New Delhi, India, 2011; Available online: https://www.nbmcw.com/tech-articles/concrete/25796-strength-of-concrete-vs-grades-of-cement.html (accessed on 1 May 2021).
15. Ji, Z.; Pei, Y. Bibliographic and visualized analysis of geopolymer research and its application in heavy metal immobilization: A review. *J. Environ. Manag.* **2019**, *231*, 256–267. [CrossRef] [PubMed]
16. Zhang, Y.; Wei, S.; Qianli, C.; Lin, C. Synthesis and heavy metal immobilization behaviors of slag based geopolymer. *J. Hazard. Mater.* **2007**, *143*, 206–213. [CrossRef]
17. Rasaki, S.A.; Bingxue, Z.; Guarecuco, R.; Thomas, T.; Minghui, Y. Geopolymer for use in heavy metals adsorption, and advanced oxidative processes: A critical review. *J. Clean. Prod.* **2019**, *213*, 42–58. [CrossRef]
18. Luukkonen, T.; Tolonen, E.-T.; Runtti, H.; Kemppainen, K.; Perämäki, P.; Rämö, J.; Lassi, U. Optimization of the metakaolin geopolymer preparation for maximized ammonium adsorption capacity. *J. Mater. Sci.* **2017**, *52*, 9363–9376. [CrossRef]
19. Siyal, A.A.; Shamsuddin, M.R.; Khan, M.I.; Rabat, N.E.; Zulfiqar, M.; Man, Z.; Siame, J.; Azizli, K.A. A review on geopolymers as emerging materials for the adsorption of heavy metals and dyes. *J. Environ. Manag.* **2018**, *224*, 327–339. [CrossRef] [PubMed]
20. Lopes, C.; Lisboa, V.; Carvalho, J.; Mateus, A.; Martins, L. Challenges to access and safeguard mineral resources for society: A case study of kaolin in Portugal. *Land Use Policy* **2018**, *79*, 263–284. [CrossRef]
21. Santos, I.; Costa, C.; Quintela, A.; Terroso, D.; Ferraz, E.; Rocha, F.; Dorzhieva, O.; Krupskaya, V.; Vigasina, M. Mineralogical composition of sedimentary and residual kaolin deposits from Portugal. *Comun. Geológicas* **2014**, *101*, 195–197.

22. Andrejkovičová, S.; Sudagar, A.; Rocha, J.; Patinha, C.; Hajjaji, W.; Ferreira da Silva, E.; Velosa, A.; Rocha, F. The effect of natural zeolite on microstructure, mechanical and heavy metals adsorption properties of metakaolin based geopolymers. *Appl. Clay Sci.* **2016**, *126*, 141–152. [CrossRef]
23. Sudagar, A.; Andrejkovičová, S.; Patinha, C.; Velosa, A.; McAdam, A.; Da Silva, E.F.; Rocha, F. A novel study on the influence of cork waste residue on metakaolin-zeolite based geopolymers. *Appl. Clay Sci.* **2018**, *152*, 196–210. [CrossRef]
24. *Methods of Test. for Mortar for Masonry—Part 11: Determination of Flexural and Compressive Strength of Hardened Mortar*; BSI: London, UK, 1999.
25. Cadar, O.; Senila, M.; Hoaghia, M.-A.; Scurtu, D.; Miu, I.; Levei, E.A. Effects of Thermal Treatment on Natural Clinoptilolite-Rich Zeolite Behavior in Simulated Biological Fluids. *Molecules* **2020**, *25*, 2570. [CrossRef]
26. Cheng, T.; Lee, M.; Ko, M.; Ueng, T.; Yang, S. The heavy metal adsorption characteristics on metakaolin-based geopolymer. *Appl. Clay Sci.* **2012**, *56*, 90–96. [CrossRef]
27. Zhong, Q.-Q.; Yue, Q.-Y.; Gao, B.-Y.; Li, Q.; Xu, X. A novel amphoteric adsorbent derived from biomass materials: Synthesis and adsorption for Cu(II)/Cr(VI) in single and binary systems. *Chem. Eng. J.* **2013**, *229*, 90–98. [CrossRef]
28. Kara, I.; Yilmazer, D.; Akar, S.T. Metakaolin based geopolymer as an effective adsorbent for adsorption of zinc(II) and nickel(II) ions from aqueous solutions. *Appl. Clay Sci.* **2017**, *139*, 54–63. [CrossRef]
29. Kesraoui-Ouki, S.; Cheeseman, C.; Perry, R. Effects of conditioning and treatment of chabazite and clinoptilolite prior to lead and cadmium removal. *Environ. Sci. Technol.* **1993**, *27*, 1108–1116. [CrossRef]
30. Ćurković, L.; Cerjan-Stefanović, Š.; Filipan, T. Metal ion exchange by natural and modified zeolites. *Water Res.* **1997**, *31*, 1379–1382. [CrossRef]
31. Ouki, S.K.; Kavannagh, M. Performance of Natural Zeolites for the Treatment of Mixed Metal-Contaminated Effluents. *Waste Manag. Res.* **1997**, *15*, 383–394. [CrossRef]
32. Choi, H.-J.; Yu, S.-W.; Kim, K.H. Efficient use of Mg-modified zeolite in the treatment of aqueous solution contaminated with heavy metal toxic ions. *J. Taiwan Inst. Chem. Eng.* **2016**, *63*, 482–489. [CrossRef]
33. Günay, A.; Arslankaya, E.; Tosun, I. Lead removal from aqueous solution by natural and pretreated clinoptilolite: Adsorption equilibrium and kinetics. *J. Hazard. Mater.* **2007**, *146*, 362–371. [CrossRef] [PubMed]
34. Srivastava, S.K.; Tyagi, R.; Pant, N.; Pal, N. Studies on the removal of some toxic metal ions. Part II (removal of lead and cadmium by montmorillonite and kaolinite). *Environ. Technol. Lett.* **1989**, *10*, 275–282. [CrossRef]
35. Jiang, M.-Q.; Jin, X.-Y.; Lu, X.-Q.; Chen, Z.-L. Adsorption of Pb(II), Cd(II), Ni(II) and Cu(II) onto natural kaolinite clay. *Desalination* **2010**, *252*, 33–39. [CrossRef]
36. Al-Harahsheh, M.; Shawabkeh, R.; Al-Harahsheh, A.; Tarawneh, K.; Batiha, M.M. Surface modification and characterization of Jordanian kaolinite: Application for lead removal from aqueous solutions. *Appl. Surf. Sci.* **2009**, *255*, 8098–8103. [CrossRef]
37. Bhattacharyya, K.G.; Gupta, S.S. Adsorptive Accumulation of Cd(II), Co(II), Cu(II), Pb(II) and Ni(II) Ions from Water onto Kaolinite: Influence of Acid Activation. *Adsorpt. Sci. Technol.* **2009**, *27*, 47–68. [CrossRef]
38. Erdem, E.; Karapinar, N.; Donat, R. The removal of heavy metal cations by natural zeolites. *J. Colloid Interface Sci.* **2004**, *280*, 309–314. [CrossRef]
39. Panayotova, M. Kinetics and thermodynamics of copper ions removal from wastewater by use of zeolite. *Waste Manag.* **2001**, *21*, 671–676. [CrossRef]
40. Alvarez-Ayuso, E.; Garcia-Sanchez, A.; Querol, X. Purification of metal electroplating waste waters using zeolites. *Water Res.* **2003**, *37*, 4855–4862. [CrossRef] [PubMed]
41. Sljivic, M.; Smiciklas, I.; Pejanovic, S.; Plecas, I. Comparative study of Cu^{2+} adsorption on a zeolite, a clay and a diatomite from Serbia. *Appl. Clay Sci.* **2009**, *43*, 33–40. [CrossRef]
42. Yavuz, Ö.; Altunkaynak, Y.; Güzel, F. Removal of copper, nickel, cobalt and manganese from aqueous solution by kaolinite. *Water Res.* **2003**, *37*, 948–952. [CrossRef]
43. El-Eswed, B.; Yousef, R.I.; Alshaaer, M.; Hamadneh, I.; Khalili, F. Adsorption of Cu(II), Ni(II), Zn(II), Cd(II) and Pb(II) onto kaolin/zeolite based-geopolymers. *Adv. Mater. Phys. Chem.* **2012**, *2*, 119–125. [CrossRef]
44. Chai, W.; Huang, Y.; Su, S.; Han, G.; Liu, J.; Cao, Y. Adsorption behavior of Zn(II) onto natural minerals in wastewater A comparative study of bentonite and kaolinite. *Physicochem. Probl. Miner. Process.* **2016**, *53*, 264–278.
45. Gupta, S.S.; Bhattacharyya, K.G. Removal of Cd(II) from aqueous solution by kaolinite, montmorillonite and their poly(oxo zir-conium) and tetrabutylammonium derivatives. *J. Hazard. Mater.* **2006**, *128*, 247–257. [CrossRef]